Journal of Science and Mathematics Letters, Vol 6, 2018 (32-46)
ISSN 2462-2052, eISSN 2600-8718

RESEARCH PAPER

The Structural, Physical and Optical Properties of Borotellurite Glasses Incorporated with Silica from Rice Husk

Umar Saad Aliyu,[1,2*], Halimah Mohamed Kamari[1], Abdulkarim Muhammad Hamza[1,3], Abdulbaset Abdulla Awshah[1]

[1]Department of Physics, Faculty of Science, Universiti Putra Malaysia, 43400 UPM Serdang, Selangor, Malaysia
[2]Department of Physics, Faculty of Science, Federal University Lafia, Nigeria
[3]National Agency for Science and Engineering Infrastructure, Abuja, Nigeria

[*]Corresponding author: usaltilde@yahoo.com

Received: 10 November 2018; Accepted: 5 December 2018; Published: 15 December 2018

Abstract

From the agricultural waste of rice (rice husk), high purity SiO_2 with about 98.548 % purity was extracted using a very simple room temperature leaching method. Using the rice husk extracted silicate, a system of silicate borotellurite glasses was fabricated with composition equation $[(TeO_2)_{0.7}\ (B_2O_3)_{0.3}]_{1-x}\ (SiO_2)_x$ with x= 0.0, 0.1, 0.2, 0.3 and 0.4. The density and molar volume were measured, and Fourier transform infrared (FTIR), X-ray diffraction (XRD) and UV-Vis analyses were performed on the glasses. Both the density and molar volume decreased and the XRD pattern confirmed the glasses' amorphous nature. The FTIR showed the presence of TeO_3, TeO_4, BO_3, BO_2O, SiO_4, and H_3BO_3 structural units in the glasses. The concentrations of TeO_3, TeO_4, BO_3 and BO_2O structures were determined by the deconvolution of the FTIR spectra using an Origin software. The optical energy band gap, index of refraction, oxygen packing density (OPD), molar refractive index, metallization criterion and polaron radius were determined for the glasses. Based on the glass transparency, high refractive index value (2.3026 and 2.2937) and metallization criterion (0.4109 and 0.4132) of the glasses with x= 0.1 and 0.2 have potential for fiber and optical non-linear applications.

Keywords: Cold leaching, Rice husk ash, Borotellurite, Refractive index

Abstrak

Daripada sisa pertanian sekam padi (rice husk), keaslian SiO_2 pada 98.548% ketulenan diekstrak menggunakan larut lesap pada suhu bilik. Menggunakan sekam padi yang telah diekstrak silikat, sistem kaca borotellurit silikat telah dihasilkan dengan komposisi [(TeO2) (B2O3) 0.7 0.3] 1-x (SiO2) x x = 0.0, 0.1, 0.2, 0.3 dan 0.4. Ketumpatan dan isipadu molar diukur, dan inframerah Fourier (FTIR), belauan sinar-X (XRD) dan analisis UV-Vis pada kaca dibentangkan. Ketumpatan dan isipadu molar yang menurun dan corak XRD mengesahkan sifat amorfus kaca. FTIR menunjukkan kewujudan unit struktur TeO3, TeO4, BO3, BO2O, SiO4, dan H3BO3 dalam kaca. Kepekatan struktur TeO3, BO3, TeO4 dan BO2O telah ditentukan nyahkonvolusi FTIR dengan menggunakan perisian Origin. Tenaga jurang optik, indeks pembiasan cahaya, kemampatan oksigen, indeks biasan molar, kriteria kelogaman dan radius polaron telah ditentukan bagi kaca. Berdasarkan kaca lutsinar, nilai indeks biasa adalah tinggi (2.3026 dan 2.2937) dan kriteria kelogaman (0.4109 dan 0.4132) kaca dengan x = 0.1 dan 0.2 mempunyai potensi untuk fiber dan aplikasi optik tidak linear.

Kata kunci: Larut lesap sejuk, Debu sekam padi, Borotellurit, Borotellurit

INTRODUCTION

The rice husk constitute 22% of the rice paddy mass, composition of each constituent as 25% Hemicellulose, 35% cellulose, 3% Crude protein, 20% lignin and 17% Ash (silica) (Ugheoke & Mamat, 2012). The rice husk silicate utilization in the fabrication of transparent materials for radiation protection applications was reported by Mustafa and coworkers. Hot leaching method was used in the extraction of SiO_2 from the rice husk (Mustafa et al., 2012).

Over the recent decades, the utilization of TeO_2 in various glass applications has become the interest of both scientists and industrialist. Although a conditional glass former, tellurium oxide is considered in the fields of glass science and technology because it provides high index of refraction, good rare-earth ions solubility that ensures high efficiency for hosting rare-earth ions (dopants) which allows an environment for radiative transition (Kaur, 2015; Mustafa et al., 2015). They also have the lowest phonon energy among the other oxide glass formers. Tellurite glasses are relatively easier to fabricate due to their low glass transition temperature and low melting point when compared to other glass families (Gaafar et al., 2011).

The combination of boron oxide and tellurium oxide in the glass science and technology provided the advantage of exploring the boron oxide's advantages of high rare earth ion solubility, low melting temperature, hardness and transparency (Mustafa et al., 2015). According to Hasnimuliyati et al., incorporation of B_2O_3 into tellurite glass system produces a structural unit that is interesting and enhances the physical and optical quality of the glasses through density decrease and IR transmission enhancement (Hasnimulyati et al., 2017).

This work aimed at utilizing the silicon oxide from the agricultural waste of rice called rice husk for the possible improvement of the physical, optical and structural quality of borotellurite glass system for optical fibre and photonic applications. This is expected to be an alternative waste management solution to the environment pollution the disposition of the waste might have caused the neighbouring communities. X-ray diffraction (XRD) and Fourier Transform infrared (FTIR) spectroscopic analysis was used for the confirmation of the crystalline or otherwise nature and the structural changes in the glass network. Density and molar volume were determined to study the physical properties of the glasses. UV-vis was used to study the optical and other physical properties which includes the optical band gap energy, Urbach energy, refractive index, molar refractive index, transmission coefficient, reflection loss and polaron radius.

MATERIALS AND METHODS

Silicate Extraction

The required amount of rice husk for silicon extraction was put in a plastic bowl and washed with water at room temperature three times with the aim of removing dusts and other dirt-based impurities. Using a plastic bowl sieve, the rice husk was sieved to allow the dirt and dust drain out of the rice husk for the three washing sessions. The washed rice husk was then soaked in a 2 M HCl solution for a two-hour leaching at room temperature without heating. The essence of the acid leaching was the dissolve and remove all acid soluble metal oxides and compounds within and around the fabrics of the rice husk. The leached and drained rice husk was then washed using deionized water to free the rice husk fabrics from the acid. The deionized water washed rice husk was then drained off the water in a bowl sieved for 24 hours and then dried using an electric oven for 4 hours at 120 ^{o}C. The dried

rice husk was then burned at 600 ^{o}C to form a white ash. The white coloured rice husk ash is the SiO_2 extracted.

Glass Fabrication

Using the extracted SiO_2 (RHA, 98.548%), B_2O_3 (Alfar Aeser) and TeO_2 (Alfar Aeser), samples of glasses were prepared based on the compositional formula $[(TeO_2)_{0.7}\ (B_2O_3)_{0.3}]_{1-x}\ (SiO_2)_x$ with x= 0.0, 0.1, 0.2, 0.3 and 0.4 by using the melt-quenching technique. Using a high precision balance, each chemical component was weighed based on its compositional proportion in the formula and mixed together in a cleaned alumina crucible. To make the mixtures homogeneous, the chemicals were stirred for about 30 minutes. The stirred chemical mixture in the crucible was put in an electric furnace at 400 ^{o}C and allowed for one hour for pre-heating and then moved to another electric furnace set at temperature range of 900 ^{o}C - 1150 ^{o}C (depending on the SiO2 proportion in the mixture) for 1 to 2 hours for melting of samples. The temperature and heating time requirement for melting increased as the amount of RHA (SiO_2) was increased. The mixture melt was then turned into a cylindrical mold preheated at 400 ^{o}C for casting and transferred back to the furnace at 400 ^{o}C. The melt in the mold was then allowed for another 1 hour for annealing and solidification. The annealing of the glass sample was to ensure bubbles and thermal stress are removed (Salah, 2018). The glasses were cut into 2 mm thickness and to achieve parallelism of the glass surfaces, the glasses were polished using silicon carbide. A portion of the glass samples were crushed to fine powdered form for the XRD and FTIR analyses.

Measurements and Characterizations

The density of the glass samples prepared in this study was measured using the electronic densimeter MD-300 model (precision = 0.001g), with the capacity of measuring up to 300 g by Alfa Mirage company. The device works on the Archimedes principle by liquid suspension. The immersion liquid used was distilled water and all measurements carried out under normal ambient conditions.

The samples' density (ρ_s) calculations was carried out using the formula reported by (Awshah, 2017) as;

$$\rho_s = \frac{W_A}{W_w}\rho_w \quad (1)$$

The calculation of the values of the molar volume (M_V) was performed using the expression;

$$M_V = \frac{M_W}{\rho_s} \quad (2)$$

Where W_A, W_w, ρ_w, and M_W are the sample's weight in air, in water, water density and the molar weight of the sample respectively (Mustafa et al., 2015).

In this work, the compositional analysis of the rice husk ash was carried out using Shimadzu Energy Dispersion X-Ray Spectrometer (EDX-720). XRD analysis of all the samples (Powdered) in the experiment was run for 2θ values between 20^{o} to 80^{o} at a minimum step size of 0.01^{o}.

The Perkin Elmer 1650 spectrometer was used in collecting and recording the FTIR spectra in the energy range of 200 – 4000 cm^{-1} at ambient condition. The UV-Vis analysis is used in the study of the optical and structural properties of materials. The optical absorption spectra for the polished glass samples (2.00 mm thickness) were obtained at room

temperature using UV–Visible spectrometer (Shidamatsu Model UV-1650PC) in the wavelength range from 200-1000 nm.

RESULTS AND DISCUSSION

The result of the XRF analysis performed on the extracted SiO_2 as shown in Table 1 indicates high purity of about 98.548%. The purity of the extracted silicate is basically dependent on many different factors which includes; the soil nature of the area where the rice was produced, the rice variety, leaching acid concentration and temperature and burning temperature of the husk (Umar et al., 2017).

Table 1. The XRF analysis result showing the various elements/oxides and their concentrations in the RHA

Element (Oxide)	Amount /Percentage (%)
SiO_2	98.548
SO_3	0.793
CaO	0.407
Fe_2O_3	0.129
K_2O	0.079
MnO	0.035
ZnO	0.009

Figure 1 presents the result of the XRD for the $[(TeO_2)_{0.7}\ (B_2O_3)_{0.3}]_{1-x}\ (SiO_2)_x$ glass system in the range of $20^o \leq 2\theta \geq 80^o$. The pattern showed no sharp peaks but only a broad hump around $20^o < 2\theta < 30^o$. The broad hump confirmed the non-crystallinity (amorphous nature) of the glasses (Hasnimulyati et al., 2017). The presence of a minor peak is due to the presence of a crystalline phase of tellurium oxide (α-TeO_2) formed in the glass structure (Munoz-Martín et al., 2009).

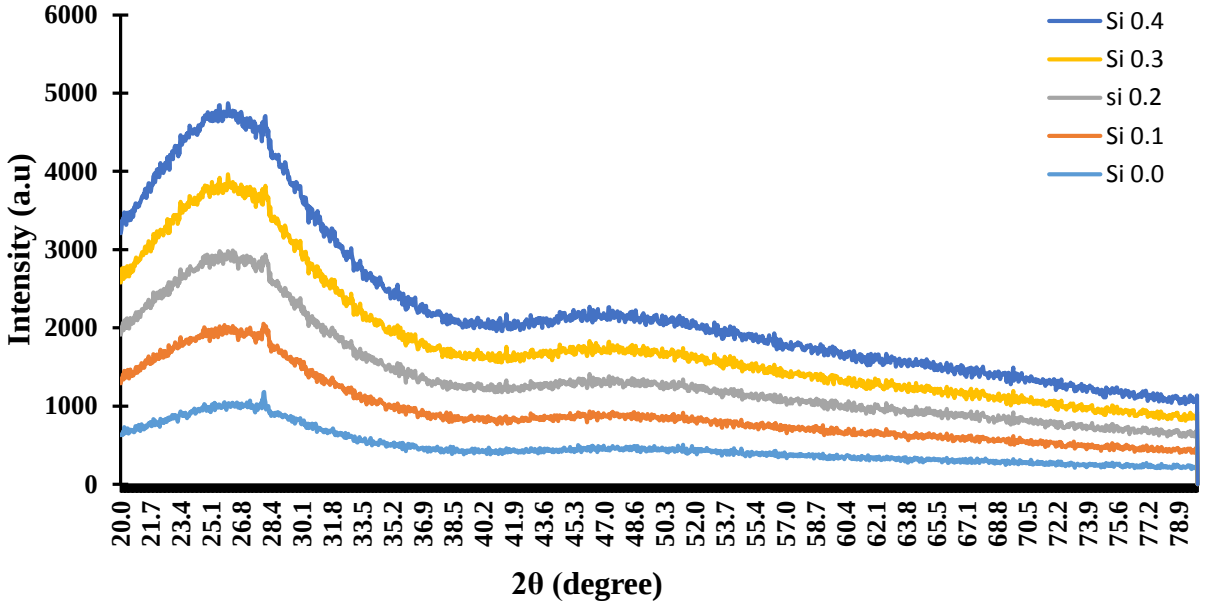

Figure 1. The XRD pattern of $[(TeO_2)_{0.7}\ (B_2O_3)_{0.3}]_{1-x}\ (SiO_2)_x$ glass system

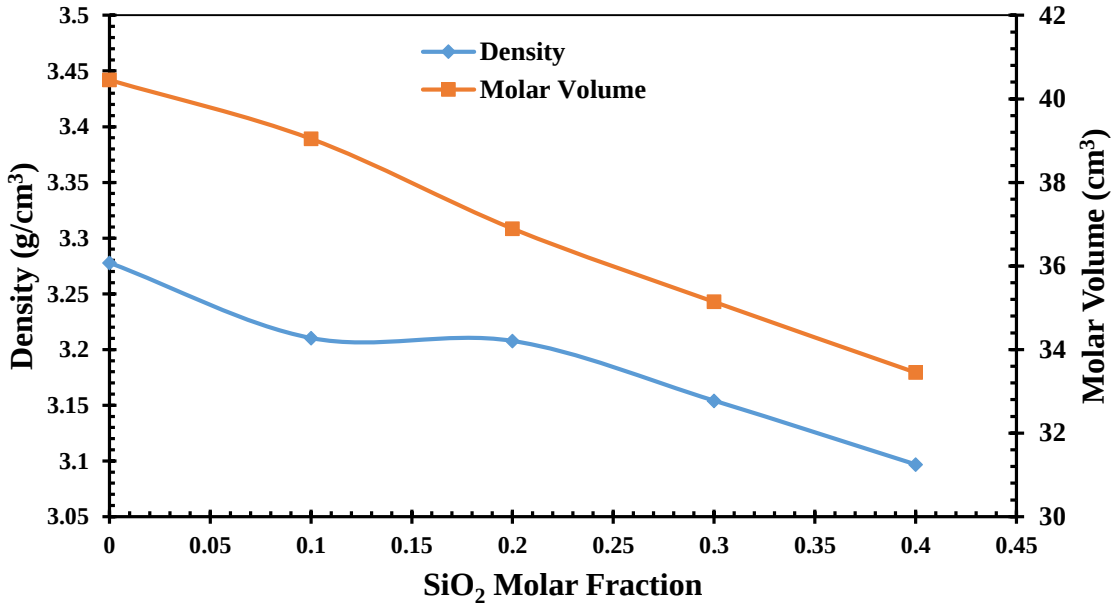

Figure 2. Density and molar volume variation with molar fraction of SiO_2 in $[(TeO_2)_{0.7}\ (B_2O_3)_{0.3}]_{1-x}\ (SiO_2)_x$ glass system

The density and molar volume variation with SiO_2 molar fraction in $[(TeO_2)_{0.7}\ (B_2O_3)_{0.3}]_{1-x}\ (SiO_2)_x$ glass system is presented in Figure 2. The density value decreased from 3.2779 to 3.0968 g cm^{-3} and the molar volume value decreased from 40.4547 to 33.4520 cm^3/mol as the SiO_2 molar concentration increase from 0 to 40%. The decrease in the density value maybe ascribed to the substitution denser Te (127.60 amu) atoms with lighter Si (60.08 amu) atoms, thereby making the resulting glass molecular weight to decrease (Umar et al., 2017). The decrease in the molar volume of the glasses might be due to the substitution of Te atoms having larger atomic radius (140 pm) with Si atoms that have smaller atomic radius (111 pm), thereby decreasing the space coverage of the atoms (Mustafa et al., 2015). The decrease may also be associated with the increase in the formation TeO_4 structural unit

which forms more crosslinks between cations and the oxygen atoms in the glass network (Abdulbaset et al., 2017).

Figure 3 presents the FTIR spectra of the $[(TeO_2)_{0.7}\ (B_2O_3)_{0.3}]_{1-x}\ (SiO_2)_x$ glass system. About six absorption bands were observed, with peak centers around 550-640 cm^{-1}, 650-700 cm^{-1}, 950-1150 cm^{-1}, 1220-1240 cm^{-1}, 1350-1378 cm^{-1} and one band from sample 0.0% SiO_2 with peak around 3200 cm^{-1}. The bands with peak centers around 550-640 cm^{-1}, 650-700 cm^{-1}, 950-1150 cm^{-1}, 1220-1240 cm^{-1}, 1350-1378 cm^{-1} and around 3200 cm^{-1} are ascribed to Te-O bond vibrations between the trigonal bipyramid unit (TeO_4) and the bridging oxygen atom (Battisha & Nahrawy, 2012), Te-O bond asymmetric vibrations in the TeO_3 units (Putra et al., 2013), S-O-Si asymmetric stretching of the bridging oxygen atoms of silica (Battisha & Nahrawy, 2012), Stretching vibrations of B-O in the BO_3 units in boroxol rings (Azuraida, 2015), Asymmetric stretching modes of borate triangles $B\Theta_3$, $B\Theta_2O$ with NBO (Rodriguez, 2016) and O-H group vibration in H_3BO_3 units (Hesham & Samier, 2013) respectively.

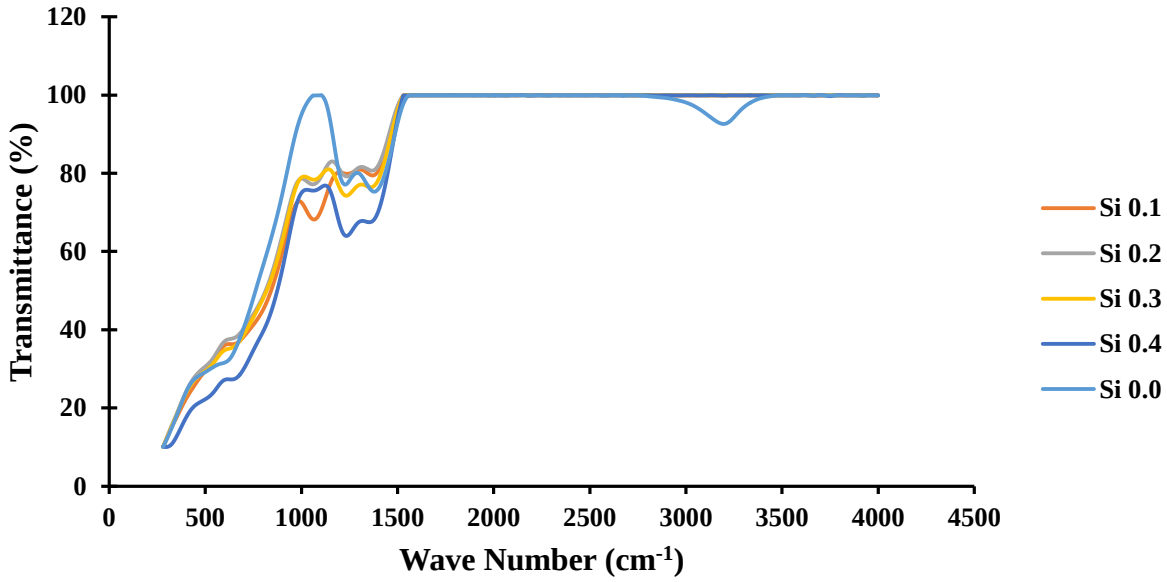

Figure 3. The FTIR spectra of the $[(TeO_2)_{0.7}\ (B_2O_3)_{0.3}]_{1-x}\ (SiO_2)_x$ glass system

Table 2. Relative Areas of the Deconvoluted FTIR Peaks Assigned to TeO_4, TeO_3, BO_3 and $B\Theta_3$ /$B\Theta_2O$ in $[(TeO_2)_{0.7}\ (B_2O_3)_{0.3}]_{1-x}\ (SiO_2)_x$ glass system

X	TeO_4	TeO_3	BO_3	$B\Theta_3$ /$B\Theta_2O$
0	190.82	109.39	10.781	23.711
0.1	45.94	132.61	13.871	18.837
0.2	66.495	124.32	12.88	16.559
0.3	96.467	101.33	12.572	14.629
0.4	121.521	89.64	11.199	9.088

The FTIR spectral deconvolution results showing the concentrations of various structural units in the $[(TeO_2)_{0.7}\ (B_2O_3)_{0.3}]_{1-x}\ (SiO_2)_x$ glass system is shown in Table 3. The initial decrease in the TeO_4 concentration with the first introduction of SiO_2 introduction lead to an increase in the formation of more TeO_3. TeO_4 and TeO_3 are associated with increase in bridging and non-bridging oxygens respectively (Umar et al., 2017). The BO_3 structural units are divided into two, one with all bridging oxygen and the other with a single non-bridging oxygen assigned as BO_3 and BO_2O respectively (Rodriguez, 2016).

The UV-Vis absorption spectra of $[(TeO_2)_{0.7}\ (B_2O_3)_{0.3}]_{1-x}\ (SiO_2)_x$ glass system as presented in Figure 4 for wavelengths range between 200 -1000 nm. The spectra showed no absorption peaks indicating no rare earth ions present (El-Mallawany, 2005). The presence of not sharply defined of UV-Vis absorption edges in the spectra confirmed the amorphous nature of the glasses. The absorption spectra for samples Si 0.3 and Si 0.4 with silica concentration of 30% and 40% respectively showed different natures from the first three (3) samples (0 to 2% SiO_2 composition). This may be because from 30% silica concentration, the sample became dark.

Figure 5 and Table 4 presents the values of the direct and indirect optical band gaps for the studied $[(TeO_2)_{0.7}\ (B_2O_3)_{0.3}]_{1-x}\ (SiO_2)_x$ glass system. The values were obtained using the expression for the absorption coefficient α (υ), proposed by Davis and Mott given in equation (3).

$$\alpha(\upsilon) = B\frac{(h\upsilon - E_{opt})^n}{h\upsilon} \tag{3}$$

Where *n* (2 for indirect and ½ for direct) is a number and B is a constant. The value of α(υ) is the absorption coefficient obtained using the expression;

$$\alpha(\upsilon) = 2.303\frac{A}{t} \tag{4}$$

where *t* is the sample thickness, A is the value of the corresponding optical absorbance for a sample.

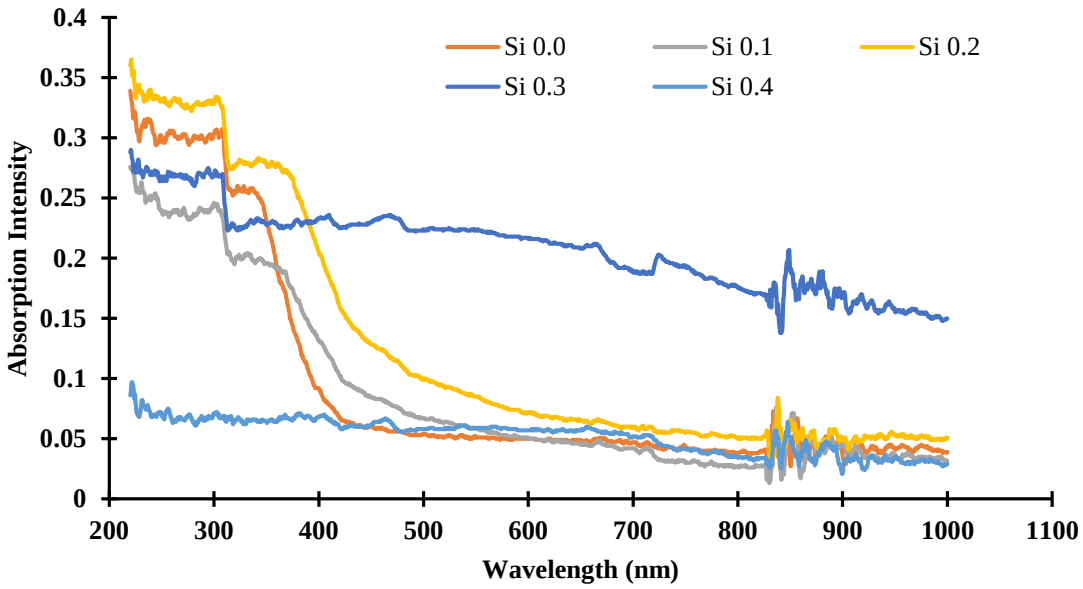

Figure 2. The UV-Vis Absorption Spectra of $[(TeO_2)_{0.7}\ (B_2O_3)_{0.3}]_{1-x}\ (SiO_2)_x$ glass system

The 0.4 SiO_2 sample has a spectrum that could not support the band gap determination using the Davis and Mott expression due to its opaque nature and hence it was only possible to obtain the band gap values for the samples with SiO_2 concentration between 0 to 30%.

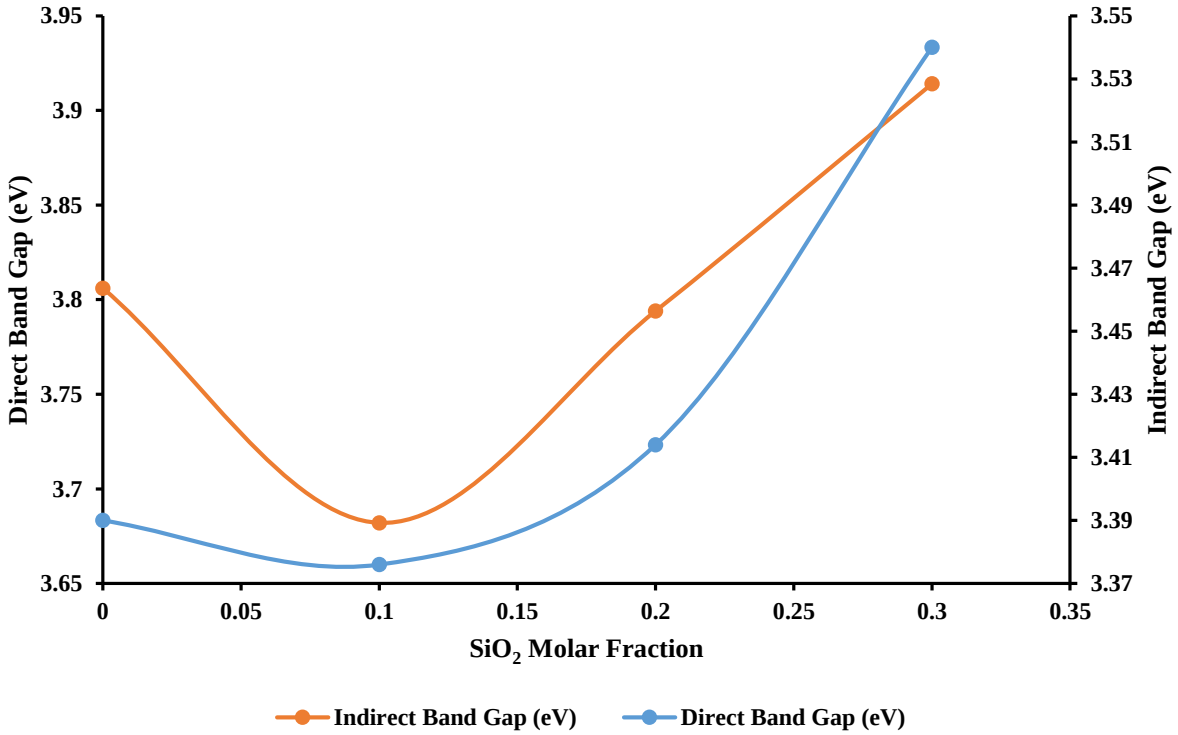

Figure 3. Variation of Energy Band Gaps (Direct and Indirect) with SiO_2 Molar Fraction in $[(TeO_2)_{0.7}(B_2O_3)_{0.3}]_{1-x}(SiO_2)_x$ glass system

The direct and indirect band gaps decreased from 3.806 to 3.682 eV and 3.39 to 3.376 eV respectively as the SiO_2 is introduced from 0.0 to 0.1 molar fraction. The value then increased up to 3.914 eV and 3.540 eV respectively as the SiO_2 concentration is increased from 0.1 to 0.3. In both cases, the initial decrease may be due to a decrease in the covalent of the glass caused by the introduction of SiO_2 which acts more as a glass former than the other components material, thereby making TeO_2 as a modifier in the glass system. This produces more non-bridging oxygen (NBO) in the glass system (Hafiz et al., 2012). The increase in the values there after may be associated with the increase in the glass network connectivity due the addition of more covalent material (SiO_2) in the glass network which thereby decreased the electrons localization degree which in turn decreases the glass matrix donor center (Pawar et al., 2017).

.

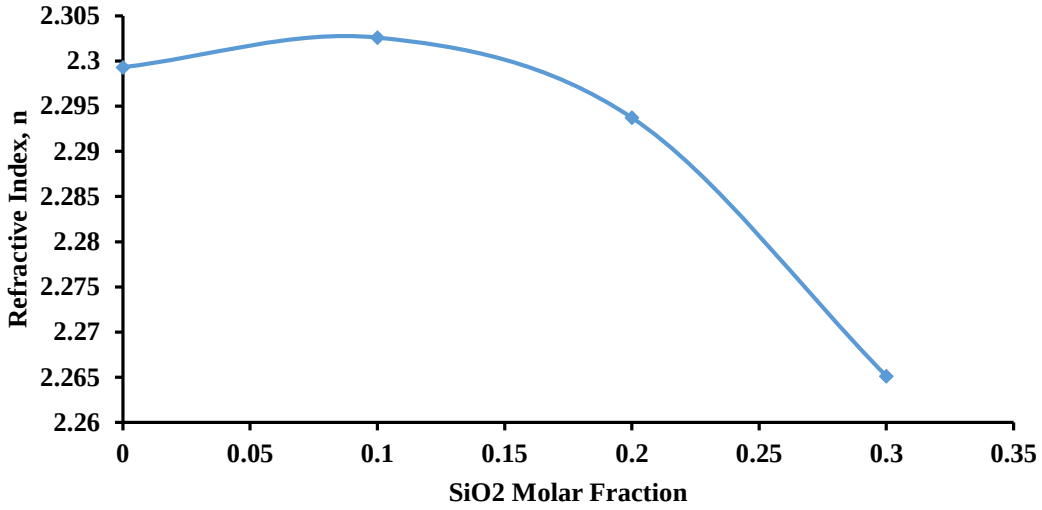

Figure 4. Variation of Refractive Index with SiO_2 Concentration in $[(TeO_2)_{0.7}\ (B_2O_3)_{0.3}]_{1-x}\ (SiO_2)_x$ glass system

Using the indirect energy band gap values, the refractive index values where obtained as reported by (Eevon et al., 2016);

$$\frac{n^2-1}{n^2+2} = 1-\sqrt{\frac{E_{opt}}{20}} \qquad (5)$$

The refractive index presented in Figure 5.6 and Table 5.4 increased from 2.2993 to 2.3026 and then decreased from 2.3036 to 2.265 as the SiO_2 concentration is increased from 0.0 to 0.1 and 0.1 to 0.3 molar fractions respectively. The initial increase in the refractive may be associated with a change in the structural arrangements of the atoms in the glass network which produces more NBO by the initial introduction of SiO_2 units in the network. This increased the polarizability of the material through the increase in the NBOs produced as a result of TeO_3 formation. NBOs are more polarizable than bridging oxygen (BOs) (Salah, 2018; Eevon et al., 2016). The decrease in the refractive index observed may be associated with the substitution of Te^{4+} ions with Si^{4+} ions which are of lower polarizability than the Te^{4+} ions (Gouraud et al., 2015). Refractive index describes the ability of a material to deviate an optical wave as it passes through the material. The refraction effect is a result of interaction between light charged particle (ions and electrons) in a material. The charged particles cause the light wave deviation and in response, the light wave (electromagnetic field of the wave) polarizes the ions and the electrons in response (Tanner, 2013) (Salah, 2018).

Table 4. Indirect Band Gap ($E^{1/2}_{opt}$), Direct Band Gap (E^{2}_{opt}), Urbach Energy (ΔE), Refractive Index (n) and Molar Refractive Index of $[(TeO_2)_{0.7}\ (B_2O_3)_{0.3}]_{1-x}\ (SiO_2)_x$ glass system

X	$E^{1/2}_{opt}$ (eV)	E^{2}_{opt} (eV)	ΔE (eV)	N (x 10^{20} cm^{-3})	R_m
0	3.39	3.806	0.4228	2.2993	23.799
0.1	3.376	3.682	0.5839	2.3026	23.004

0.2	3.414	3.794	0.4252	2.2937	21.652
0.3	3.540	3.914	1.1528	2.2651	20.358
0.4	-	-	-	2.2572	-

The Urbach energy values expressed in Table 4 increased from 0.4228 to 1.1528 eV as the SiO_2 concentration increased from 0.0 to 0.3 molar fractions. The Urbach energy in material sciences expresses the tailing of the forbidden energy in a band gap of a material (Anand Pandarinath et al., 2016). Larger Urbach energy materials usually have higher tendencies to convert weak bond to defects (Pawar et al., 2017).

The oxygen packing density as the degree of oxide network packing is calculated using an expression reported by (Gayathri, 2011);

$$OPD = X\left(\frac{\rho}{m_w}\right) \quad (6)$$

The molar refractive index (R_m) calculations from the molar volume (V_m) and the refractive index (n) was carried out using the Volf and Lorentz-Lorenz formula (Meena and Bhatia, 2016) given as;

$$R_m = \left(\frac{n^2-1}{n^2+2}\right) V_m \quad (7)$$

Metallization criterion of a material describes the material's non-metallic nature on its energy band gap basis and is obtained as reported by (Berwal et al., 2017) as

$$M = 1 - \frac{R_m}{V_m} \quad (8)$$

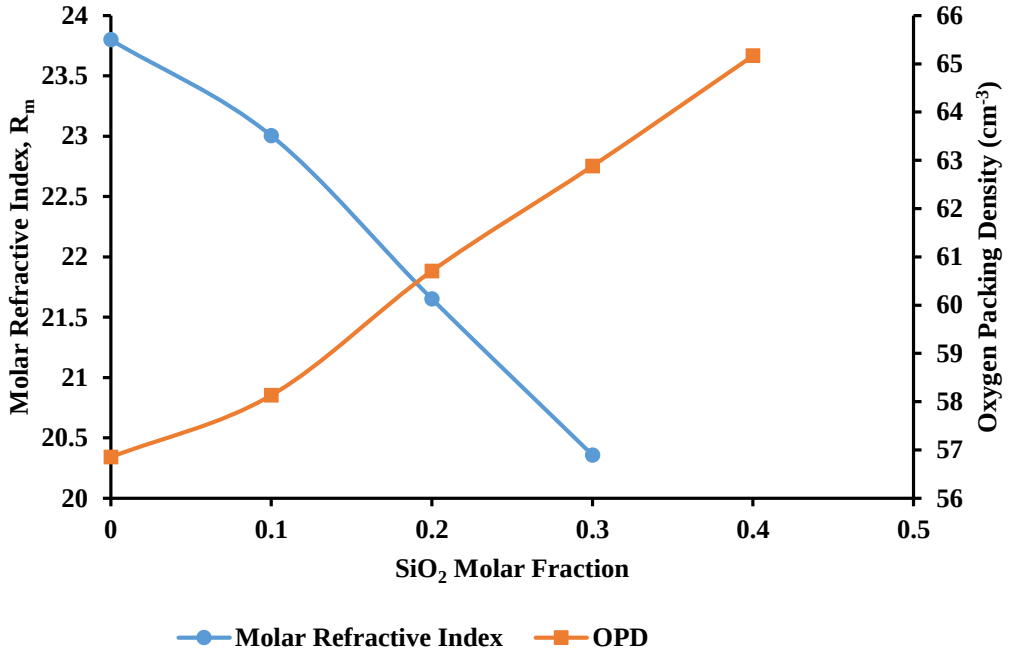

Figure 5. Variation of Molar Refractive Index and OPD with SiO_2 Molar Fraction in $[(TeO_2)_{0.7}\ (B_2O_3)_{0.3}]_{1-x}$ $(SiO_2)_x$ Glass System

Table 5. Metallization Criterion (M), Si Ion Concentration (N), Polaron Radius (R_P), Si Ion Inter-Ionic Distance (R_i) and Field Strength of Si Ion Yeild (F) for different SiO_2 molar fractions (X) in $[(TeO_2)_{0.7}\ (B_2O_3)_{0.3}]_{1-x}$ $(SiO_2)_x$ glass system

X	M	N($x10^{-21}$ cm^{-3})	R_P (Å)	R_i (Å)	F ($x10^{15}cm^2$)
0	0.4117	0	0	0	0
0.1	0.4109	1.458	7.121	8.833	2.761
0.2	0.4132	1.541	6.990	8.672	2.865
0.3	0.4208	1.605	6.896	8.555	2.944
0.4	-	1.682	6.789	8.422	3.036

The information about solid's not metallic nature is given by its metallization criterion. Oxide glasses with metallization criterion value between 0.30 to 0.45 are considered to have good optical non-linearity (Berwal et al., 2017). Metallization criterion values for $[(TeO_2)_{0.7}\ (B_2O_3)_{0.3}]_{1-x}$ $(SiO_2)_x$ glass system as presented in Table 5 increased from 0.4117 to 0.4228 with the SiO_2 concentration increased from 0.0 to 0.4. This increase is an indication of increase in the width of both the conduction and valence band which in turn widens the band gap of the material (Lakshminarayana, 2017).

The silicon ion concentration represents the number of Si^{4+} ions per unit volume of a glass system and its found using the expression reported by (Rao, 2014);

$$N = \frac{X_{Si} x\ \rho x N_A}{M_w} \quad (9)$$

where X_{Si}, N_A, ρ, and M_W represents the erbium molar fraction, Avogadro's number, density and glass sample's molar weight respectively. The inter-ionic distance of erbium ions (R_i) in the glass was calculated using the formula (Damas et al., 2012)

$$R_i\ (Å) = \frac{1}{2}\left(\frac{1}{N}\right)^{1l3} \quad (10)$$

Polaron radius in glass systems is determined using the formula reported by (Swapna, 2015) as;

$$R_p = \frac{1}{2}\left(\frac{\pi}{6N}\right)^{1/3} \quad (11)$$

The polaron radius of Si^{4+} ions in the $[(TeO_2)_{0.7}\ (B_2O_3)_{0.3}]_{1-x}\ (SiO_2)_x$ glass system as shown in Table 5 above decreased from 7.121 to 6.789 Å with increasing SiO_2 concentration from 0.1 to 0.4. The decrease in the polaron radius value may be associated with glass network connectivity and inter-ionic distance shrinkage of Si^{4+} ions in the glass system (Umar et al., 2017). Also, in Table 5, the Si ion concentration (N) increased from 1.458 x 10^{21} to 1.682 x 10^{21} cm^{-3} while R_i and F decreased and increased respectively from 8.833 to 8.422 Å and 2.761 x 10^{15} to 3.036 x 10^{15} cm^{-2} as SiO_2 concentration is increased. The increase in the R_i and F values might be associated with the increase in the material packing and average stretching force constant of the material respectively (Mhareb, 2015).

Figure 8 presents the transmission coefficient and the reflection loss of $[(TeO_2)_{0.7}\ (B_2O_3)_{0.3}]_{1-x}\ (SiO_2)_x$ glass system. The transmission coefficient increased from 0.7315 to 0.7407, while the reflection loss decreased from 0.1551 to 0.1490. The parameters T and R_L give the fraction of incident radiation transmitted and reflected respectively from the materials surface.

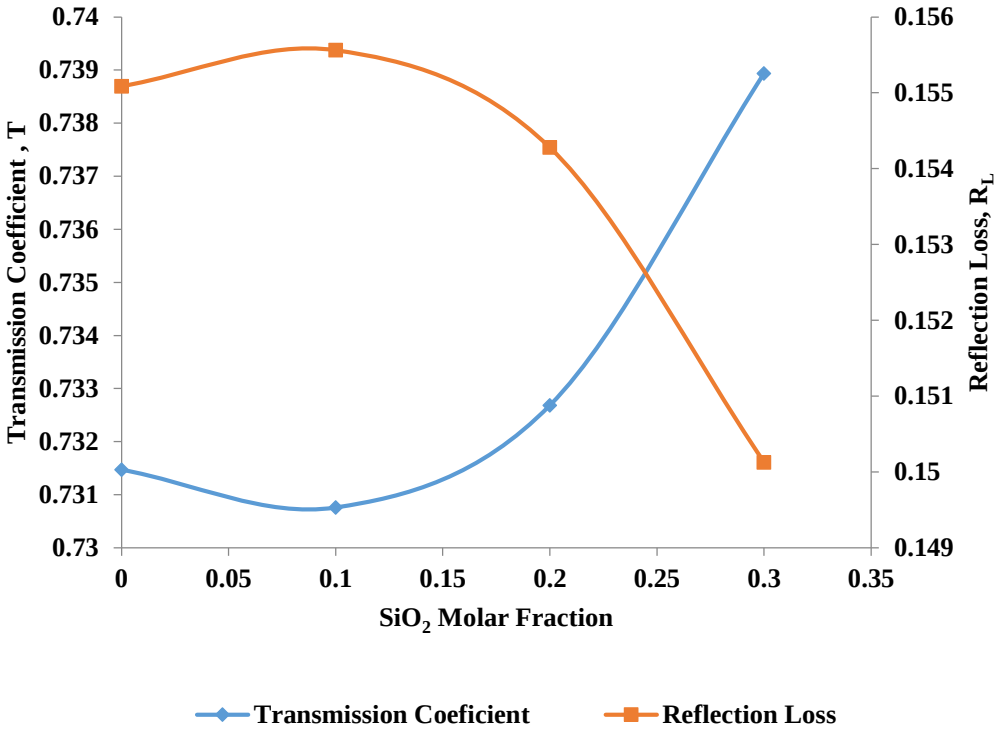

Figure 6. Transmission Coefficient (T) and Reflection Loss (R_L) with SiO_2 Molar Fraction in $[(TeO_2)_{0.7}(B_2O_3)_{0.3}]_{1-x}(SiO_2)_x$ Glass System

CONCLUSION

With about 98.548% SiO_2 purity achieved from the SiO_2 extraction from the rice husk by a very simple extraction technique (requiring no heating in leaching), a system of rice husk silicate borotellurite glasses, $[(TeO_2)_{0.7}(B_2O_3)_{0.3}]_{1-x}(SiO_2)_x$ with x = 0, 0.1, 0.2, 0.3, and 0.4 was prepared. The structural, optical and physical properties were studied using XRD, FTIR, UV-Vis characterizations and density and molar volume measurements. The glasses became dark when 30% SiO_2 was added and became darker as the percentage increased to 40%. The density and molar volume decreased with the increase in the RHA (SiO_2) concentration. The XRD pattern revealed that the glasses were all amorphous in nature. The FTIR spectra showed the presence of TeO_3, TeO_4, BO_3, BO_4, SiO_4 and H_3BO_3 structural units. The optical band gap energies decreased with the first introduction of the RHA and increased with more concentration of the RHA in the system. The refractive index increased and decreased with the introduction and further increase in the SiO_2 composition. Other parameters studied include the polarizabilities, optical basicity, reflection loss, transmission coefficient, dielectric susceptibility, metallization criterion and polaron radius. The values of the refractive index, transmission coefficient, metallization criterion and the glass transparency showed that the glasses with 10 and 20% silicate concentration have good potential for applications in fiber technology and non-linear optical applications.

ACKNOWLEDGEMENT

The authors appreciate the financial support for the work from the Minister of Higher Education of Malaysia and University Putra Malaysia through grant Putra Berimpak 9597200.

REFERENCES

Abdulbaset, A., Halimah, M.K., & Mohd Shah, N. (2017). Effect of neodymium nanoparticles on elastic properties of zinc tellurite glass system. *Advanced Materials Science Engineering, 2017,* 1-7.

Anand Pandarinath, M., Upender, G., Narasimha Rao, K., & Suresh Babu, D. (2016). Thermal, optical and spectroscopic studies of boro-tellurite glass system containing ZnO. *Journal of Non-Crystalline Solids, 433*, 60–67.

Awshah, A. A. A. (2017). Effect of neodymium nanoparticles on elastic properties of zinc-tellurite glass system. *Advanced Materials and Science Engineering, 2017*, 1-7.

Azuraida, A. (2015). Comparative studies of bismuth and barium boro-tellurite glass system: structural and optical properties. *Chalcogenide Letters, 12*(10), 497–503.

Battisha, I. & El Nahrawy, A. (2012). Physical properties of nano-composite silica-phosphate thin film prepared by sol gel technique. *New Journal of Glass Ceramics, 2,* 17–22.

Berwal, N., Dhankhar, S., Sharma, P., Kundu, R.S, Punia, S., & Kishore N. (2017). Physical, structural and optical characterization of silicate modified bismuth-borate-tellurite glasses. *Journal of Molecular Structure, 1127,* 636–644.

Damas, P., Coelho, J., Hungerford, G., & Hussain, N.S. (2012). Structural studies of lithium boro tellurite glasses doped with praseodymium and samarium oxides. *Materials Research Bulletin, 47*, 3489–3494.

Eevon, C., Halimah, M.K, Zakaria, A., Azurahanim, C.A.C, Azlan, M.N., & Faznny, M.F. (2016). Linear and nonlinear optical properties of Gd^{3+} doped zinc borotellurite glasses for all-optical switching applications. *Results in Physics Journal, 6,* 761–766.

El-Mallawany, R. (2005). An Introduction to Tellurite Glasses Module 5 – Optical Properties.

Gaafar, M. S., Abdeen, M. A. M., & Marzouk, S. Y. (2011). Structural investigation and simulation of acoustic properties of some tellurite glasses using artificial intelligence technique. *Journal of Alloys Compound, 509*(8), 3566–3575.

Gayathri Pavani, P. (2011). Optical, physical and structural studies of boro-zinc tellurite glasses. *Physica B: Physics Condensed Matter, 406*(6–7), 1242–1247.

Gouraud, F., Chotard, T., & Karray, R. (2015). Structural, mechanical and optical investigations in the TeO_2 -rich part of the TeO_2 e GeO_2 e ZnO ternary glass system. *Solid State Science, 40*, 20–30.

Hafiz, M.H.Z, Matori, K.A, Sidek, H.A.A, Zakaria, A., & Mohd Sabri, G.M. (2012). Effect of ZnO on the physical properties and optical band gap of soda lime silicate glass. *International Journal of Molecular Science, 13,* 7550–7558.

Hasnimulyati, L., Halimah, M. K., Zakaria, A., Halim, S. A., & Ishak, M. A. (2017). Comparative study of the experimental and the theoretical elastic data of Tm^{3+}doped zinc borotellurite glass. *Materials Chemistry and Physics Journal*, *192*, 228–234.

Hesham, A. & Samier, S. (2003). Ultrasonic velocity and elastic moduli of heavy metal tellurite glasses. *Materials Chemistry and Physics Journal, 80*, 517–523.

Kaur, N. (2015). Optical properties of borotellurite glasses containing metal oxides. *AIP Conference Proceedings, 070029,* 1–4.

Lakshminarayana, G. (2017). Physical, structural, thermal, and optical spectroscopy studies of TeO_2 - B_2O_3-MoO_3-ZnO-R_2O (R ¼ Li, Na, and K)/ MO (M ¼ Mg, Ca, and Pb) glasses. *Journal of Alloy and Compound, 690*, 799-816.

Meena, S.L. & Bhatia, B. (2016). Polarizability and Optical Basicity of Er^{3+} ions doped zinc lithium bismuth borate glasses. *Journal of Pure Applied Ind. Physics, 6*(10), 175–183.

Mhareb, M.H.A. (2015). Optical and erbium ion concentration correlation in lithium magnesium borate glass. *Optik (Stuttg), 126*(23), 3638–3643.

Munoz-Martín, D., Villegas, M. A., Gonzalo, J., & Fernández-Navarro, J. M. (2009). Characterisation of glasses in the TeO_2-WO_3-PbO system. *Journal of European Ceramics Society, 29*(14), 2903–2913.

Mustafa, I. S., Ain, N., Azali, N. R, Ibrahim, A. R., Yahaya, Z., & Kamari, H. M. (2015). From Rice Husk to Transparent Radiation Protection Material. *Jurnal Intelek, 9*(2), 1–6.

Pawar, P.P, Munishwar, S.R, Gautam, S., & Gedam, R.S. (2017). Physical, thermal, structural and optical properties of Dy^{3+} doped lithium alumino-borate glasses for bright W-LED. *Journal of Luminescence, 183,* 79–88.

Putra, H.S.H.S., Sidek, H.A.A, Halimah, M.K. Matori, A.W., Yusof, M.D.W., & Hafiz M.H.Z. (2013). The effect of remelting on the physical properties of borotellurite glass doped with manganese. *International Journal of Molecular Science*, *14,* 1022–1030.

Rao, Y.R. (2014). Upconversion luminescence in Er^{3+} / Yb^{3+} codoped lead bismuth indium borate glasses. *International Journal of Recent Dev. Engineering Technology, 3*(1), 2347–6435.

Rodriguez, O. (2016). Characterization of silica-based and borate-based, titanium-containing bioactive glasses for coating metallic implants. *Journal of Non-Crystalline Solids, 433,* 95–102.

Salah, H. A. (2018). Optical properties of zinc lead tellurite glasses. *Results in Physics, 9,* 1371–1376.

Swapna, K. (2015). Visible, up-conversion and NIR (1.5 μm) luminescence studies of Er^{3+} doped Zinc Alumino Bismuth Borate glasses. *Journal of Luminescence, 163*, 55–63.

Tanner, D.B. (2013). Optical effects in solids. Department of Physics, University of Florida.

Ugheoke, I. B. & Mamat, O. (2012). A critical assessment and new research directions of rice husk silica processing methods and properties. *International Journal Science Technology, 6*(3), 430–448.

Umar, S. A., Halimah, M. K., Chan, K. T., & Latif, A.A. (2017). Physical, structural and optical properties of erbium doped rice husk silicate borotellurite (Er-doped RHSBT) glasses. *Journal of Non-Crystalline Solids, 472*, 31–38.

Umar, S. A., Halimah, M. K., Chan, K. T., & Latif A. A. (2017). Polarizability, optical basicity and electric susceptibility of Er^{3+} doped silicate borotellurite glasses. *Journal of Non-Crystalline Solids, 471*, 101–109.